

Effects of Stem Design on the Mechanical Behavior of Femur with Total Hip Arthroplasty

Shun Wu¹ and Mitsugu Todo^{1,2,*}

¹Department of Molecular and Material Science, Interdisciplinary Graduate School of Engineering Sciences, Kyushu University, Japan

²Research Institute for Applied Mechanics, Kyushu University, Japan

Abstract: Total hip arthroplasty (THA) is a common orthopedic surgery, and almost only choice for those patients who suffer severe osteoarthritis. Zweymüller stem, one of the most reliable stems, is considered to be appropriate for elderly patients. However, the structural effectiveness of trochanteric shoulder for primary stability has not been clear yet. This research intended to perform a finite element analysis to explore the necessity of trochanteric shoulder for the primary stability. Realistic simulation models with a femoral bone model and three stem designs were carefully constructed. Analysis of relative sliding micromotion between bone and stem revealed that the shoulderless design has an acceptable primary stability. It was also suggested that the proximal broad design could be unnecessary for rectangular diaphyseal-fixation stems. This kind of simulation research can be an instruction to develop new design of cementless design to both achieve less invasive surgery and excellent duration.

Keyword: Cementless hip prosthesis, Primary stability, Finite element analysis.

1. INTRODUCTION

Currently, hip joint health has been one of the very concerning medical issues in the worldwide aging societies. Due to aging and other external factors such as overtaking alcohol and sterol, the processing of bone remodeling is thought to be inhibited gradually, and result in non-traumatic osteoporosis and even osteoarthritis (OA), eventually [1, 2]. Clinically, the most effective therapy for severely damaged hip joints with OA is total hip arthroplasty (THA). A typical artificial hip joint used in THA is composed of metallic stem, ceramic ball, polymeric liner and metallic acetabular cup. Among of these components, the stem plays an important role in transferring biomechanical load to femur by directly or indirectly contacting with the bone. There are two types of stems, namely, cemented stems contacting with femur through a layer of acrylic bone cement and cementless stems directly connecting with femur by osseointegration. Recently, the cementless stems have commonly been used in THA, due to their great long-term survivorship.

Mont *et al.* tried to categorize the THA stems into 6 different types on the basis of the amount of osseous contact and the location of fixation [3]. Among of them, Type 3C stem, also known as Zweymüller stem, has been well prevailing in Europe. Compared with other

designs, the characteristic design of Zweymüller stem has its unique advantages, but also some corresponding problems. It has a rectangular cross-section and tapered shape, providing great primary stability by three-point fixation at metaphyseal-diaphyseal junction and proximal diaphysis [4]. This fixation feature has let Zweymüller stem be a preferred choice for very aged patients, especially whose hips are suffering severe bone mass loss of femoral cortex at metaphyseal area.

Conventional Zweymüller stem is also known to possess an extensive shoulder, which was introduced to provide extra mechanical stability during the initial period after THA. Subsequently, the long-term stability can be achieved by bone on-growth on the porous surface of the stem. While as the fundament of long-term stability, the primary stability is susceptible to external loadings. It can raise the relative sliding motion between bone and stem, finally resulting in the failure of fixation [5, 6]. In order to introduce the shoulder, however, the proximal lateral femur have to be thinned. This increases the risk of avulsion fracture of the major trochanter. Such fracture weakens abductor and gluteal and causes thigh pain [7]. Furthermore, although a twenty-year follow-up investigation demonstrated that the survival rate of Zweymüller stem was comparable with the other cementless stems [8], this author also pointed out that the extensive proximal shoulder could be the main disadvantage because of the bone-sparing implantation. Actually, some orthopaedic surgeons think that an optimized design of stem must satisfy the condition of less invasive surgery. At the same time,

*Address correspondence to this author at the Research Institute for Applied Mechanics, Kyushu University, 6-1 Kasuga-koen, Kasuga, Fukuoka 816-8580, Japan; Tel: +81-92-583-7762; E-mail: todo@riam.kyushu-u.ac.jp

some orthopaedists doubt that the stem shoulder may not be necessary to prevent rotation and subsidence, due to the enough primary stability obtained by its characteristic three-point fixation and rectangular cross-section [7]. However, this has not been elucidated from biomechanical points of view.

The objective of the present study was to understand the effects of trochanteric shoulder of typical Zweymüller stem on the mechanical behavior of femur using CT-image based finite element analysis. CT-images of a femur was used to construct a three-dimensional femoral bone model, and CAD models of Zweymüller stems were combined with the femoral model to develop three different types of THA model. Finite element analysis was then performed to characterize the effects of stem design on the mechanical performances of the femur such as the localized energy concentration and the rotational stability.

2. METHODS

2.1. Construction of Femoral Bone Model and THA Models

CT images of a femur of 83 years-old male were used to construct a three-dimensional femoral solid model using a bone analysis software, Mechanical Finder 9.0 (RCCM, Co., Japan). Solid models of Zweymüller stem were also prepared using the corresponding CAD data of three different designs. Firstly, the head of the femoral model was incised

carefully, and then the stem models were inserted into the femoral model to simulate a realistic situation of THA. The medullary cavity was automatically created by superimposing the femoral and stem models. A ceramic ball model was also attached to the top of the stem. Three different THA models are shown in Figure 1. The three different designs of stem are called preserve α , β , and γ corresponding to shoulderless (Figs (a) and (b)), transitional (Figures (c) and (d)) and conventional design (Figures (e) and (f)), respectively.

2.2. Finite Element Analysis

Finite element models were developed using the THA models with 2 mm tetrahedron elements and 0.3 mm shell elements. The shell elements were used to express the cortical bone. The numbers of the tetrahedron and shell elements and nodes were 612,597, 22,173, and 116,375 for α model and 617,391, 22,253, and 117,645 for β model and 632,145, 22,543, and 120,913 for γ model.

Average bone mineral density (BMD) of each element was estimated assuming the linear relation between BMD values and corresponding CT values of the images. Young's modulus and the compressive yield stress of each element were then calculated from the corresponding BMD value using the empirical formulae established by Keyak, *et al.* [9]. Distributions of BMD and Young's modulus on the surface and on the cross-sectional area are shown in Figure 2. It is clearly seen that the distribution pattern is very similar

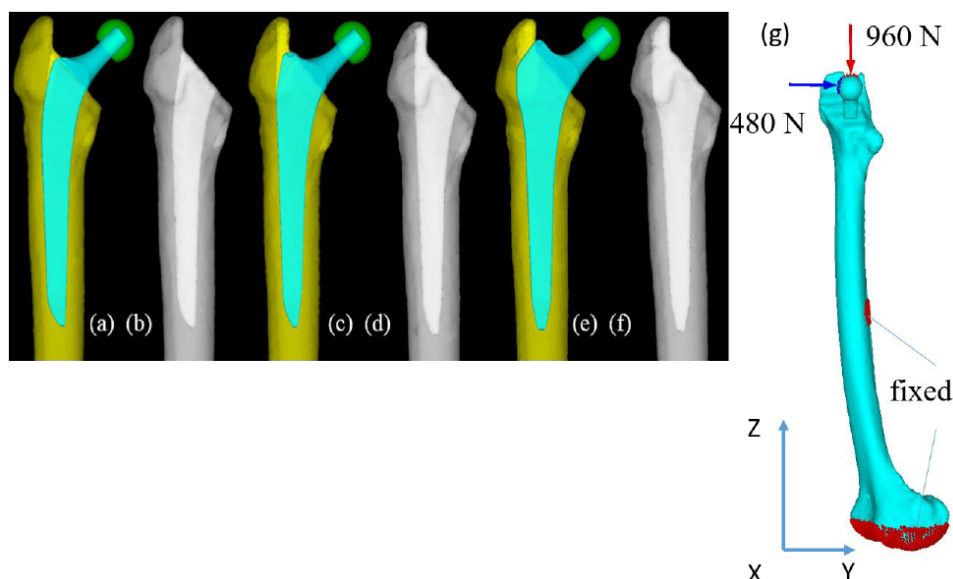


Figure 1: Scenograph of models and stems. (a) & (b) stem α , a shoulderless design; (c) & (d) stem β , a transitional design; (e) & (f) stem γ , a conventional design; (g) Loading conditions, including an axial compression of 960N and a rotational force of 480N.

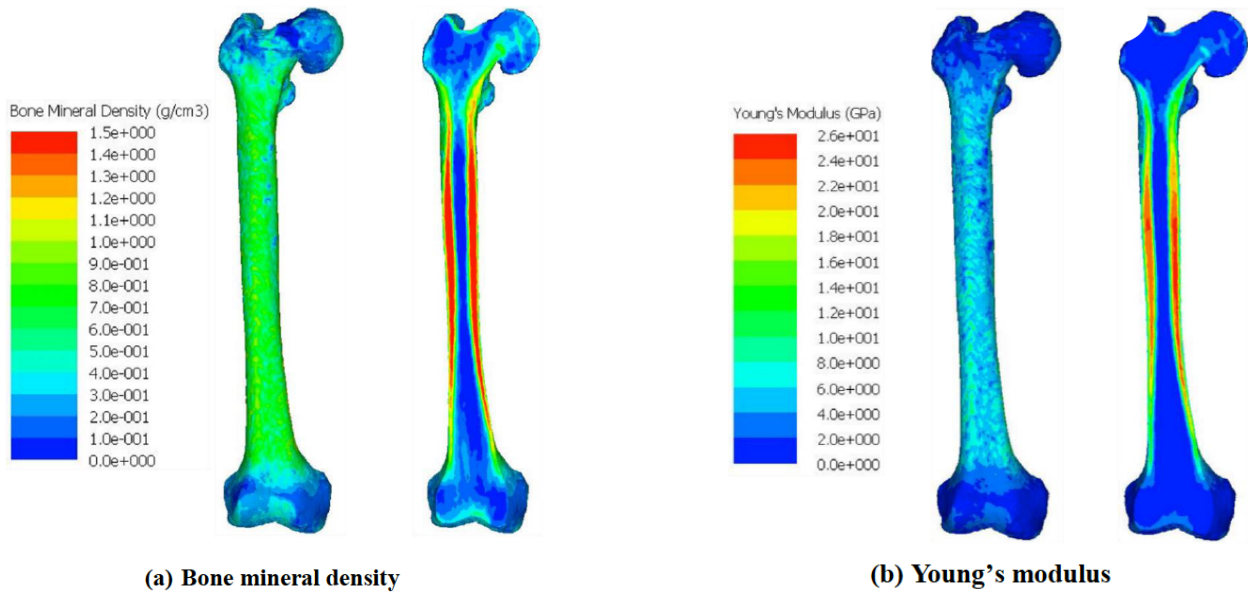


Figure 2: The distribution of (a) bone mineral density and (b) Young's modulus along the femur.

to real femur in which cortical bone has higher BMD values than porous cancellous bone. The stem and the ball were assumed to be made of titanium alloy and alumina ceramic, respectively. Young's modulus and Poisson's ratio are 114 GPa and 0.34 for titanium alloy and 370 GPa and 0.22 for alumina. The interface between bone and stem was set to satisfy a contact condition with a frictional coefficient of 0.4 to allow relative sliding motion along the interface.

The boundary conditions are also shown in Figure 1(g). The loading conditions were chosen to simulate a torsional movement under compression [10]. A vertical compressive force of 960 N was applied to the top of the ball, and a horizontal force of 480N was also

allocated to the proximal side of the ball. The distal end (condylar surface) and the middle point of the femur were totally constrained as shown in Figure 1(g). The linear elastic analysis was conducted to analyze and compare the elastic deformation behaviors of the models.

2.3. Analysis of Relative Motion

The green area shown in Figure 3(a) corresponds to the bone part in which the stem was inserted and contacted. The green and yellow areas in Figure 3(b)-(d) are the stem parts contacting the green area of bone part shown in Figure 3(a). The yellow area in Figure 3(e) indicates the bone part around the stem

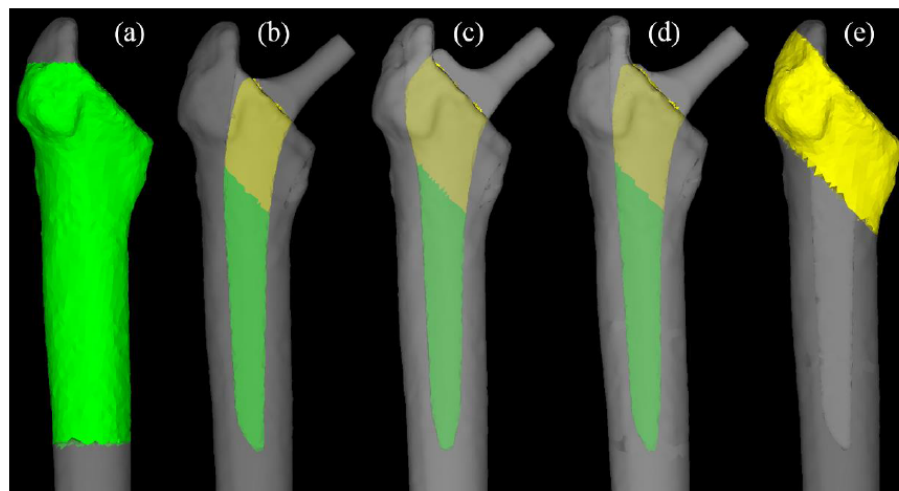


Figure 3: Illustration of selected area to calculate the displacement. (a) Green area presents bone elemented contacting with stem. (b)-(d) Green and green areas corresponded to stem elements contacting with bone. Yellow areas denoted the shoulder portion of the stem. (e) Yellow area mean the bone elements contacting with shoulder portion of stem.

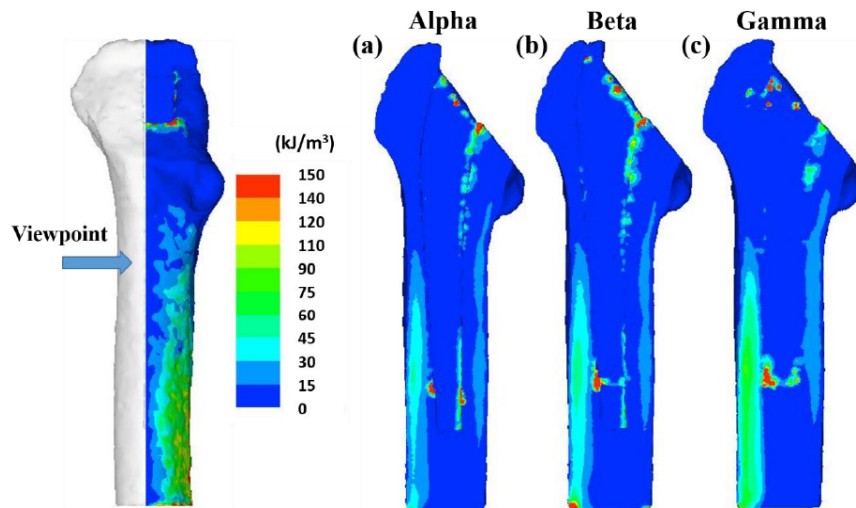
shoulder, which is the distinctive part of three stem designs. Accordingly, the yellow areas in Figure 3(b)-(d) present the stem parts around the shoulder contacting the yellow area of bone shown in Figure 3(e). The width of these oblique blocks, yellow area in Figure 3(b)-(e), is about 30 mm. The upper surfaces of the oblique blocks are parallel to the incision of the femoral neck. x, y and z-displacement components of nodes of bone and stem elements at the selected oblique blocks were obtained from the results of the finite element analysis. x and y-displacement components of a node were then used to evaluate the rotating angle of the node around the shoulder using the following formula:

$$\theta = \arctan \left[\frac{x}{y} \right] \quad (1)$$

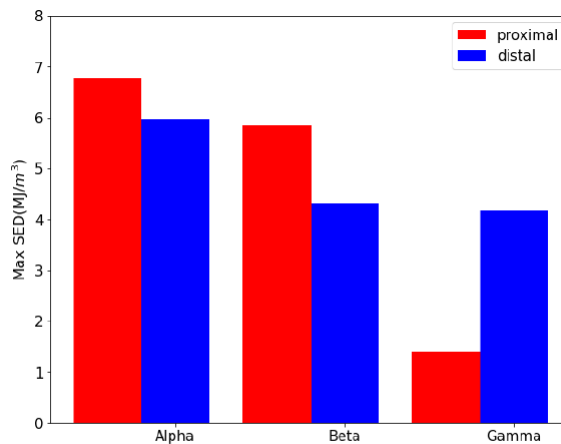
Then the average value of the rotating angles was obtained for each of the THA models. The difference between the average z-displacements of nodes of bone and stem elements in the selected areas, the whole stem (Figure 3(a)) and the shoulder region (Figure 3(e)), was defined as the relative subsidence. The relative total micromotion was also examined as the average value of the distance between bone and stem.

3. RESULTS

Distribution patterns of the strain energy density (SED) on the cross-sectional surfaces are shown in Figure 4(a). It is seen that high mechanical concentrations were generated at the points which contacted the edges of the shoulder in the proximal regions and the tips of the stems in the distal regions.



(a) Distribution of SED



(b) Maximum SED

Figure 4: Distribution and maximum values of strain energy density on the cross-sections of mid-portion.

The maximum SED values in the proximal and distal regions are also shown in Figure 4(b). Preserve α model exhibited the highest SED values of all the three designs.

The primary stability is illustrated in Figure 5 by means of the relative subsidence, rotating angle of stem and relative total micromotion around the stem shoulder during the simultaneous axial compression and torsion. The relative subsidence is the first indicator of primary stability of the whole stem contacting with bone. Preserve α model displayed the deepest subsidence of $67\mu\text{m}$ as shown in Figure 5(a). The minimum of $32\mu\text{m}$ was found in Preserve γ model. The relative subsidence increased with decreasing the width of stem shoulder. However, the relative subsidence around the stem shoulder did not perform such trend as shown in Figure 5(b). The relative subsidence around the stem shoulder of Preserve α model was close to that of Preserve γ model.

Figure 4(c) showed that the stem rotating angles were almost identical. Figure 4(d) revealed that

Preserve α model performed the largest micromotion of $138\mu\text{m}$. The minimum value of $121\mu\text{m}$ was found in Preserve β , although the difference between Preserve β and γ was $3\mu\text{m}$.

4. DISCUSSION

Sugiyama confirmed that the torsional loading could be a determinant in loosening of cementless femoral implants in THA [5, 6]. If a stem is not able to apply enough torque to arise the motion of contacting bone simultaneously, it will raise higher sliding micromotion between bone and stem. Many routine activities including leg-raising load dramatic torque on hip joints, such as up and down stairs, walking, standing up and sitting down. Bergmann verified that a 100-kilogram people can produce a torque around stem of 47 Nm without friction when stairs up [11]. Unfortunately, it was impossible in MF9.0 to observe and record stem torque, due to the restriction of the software. Hence, this study measured stem rotating angle during the torsion as an indicator of torque. Greater rotating angle was considered as the result of less torque applied at

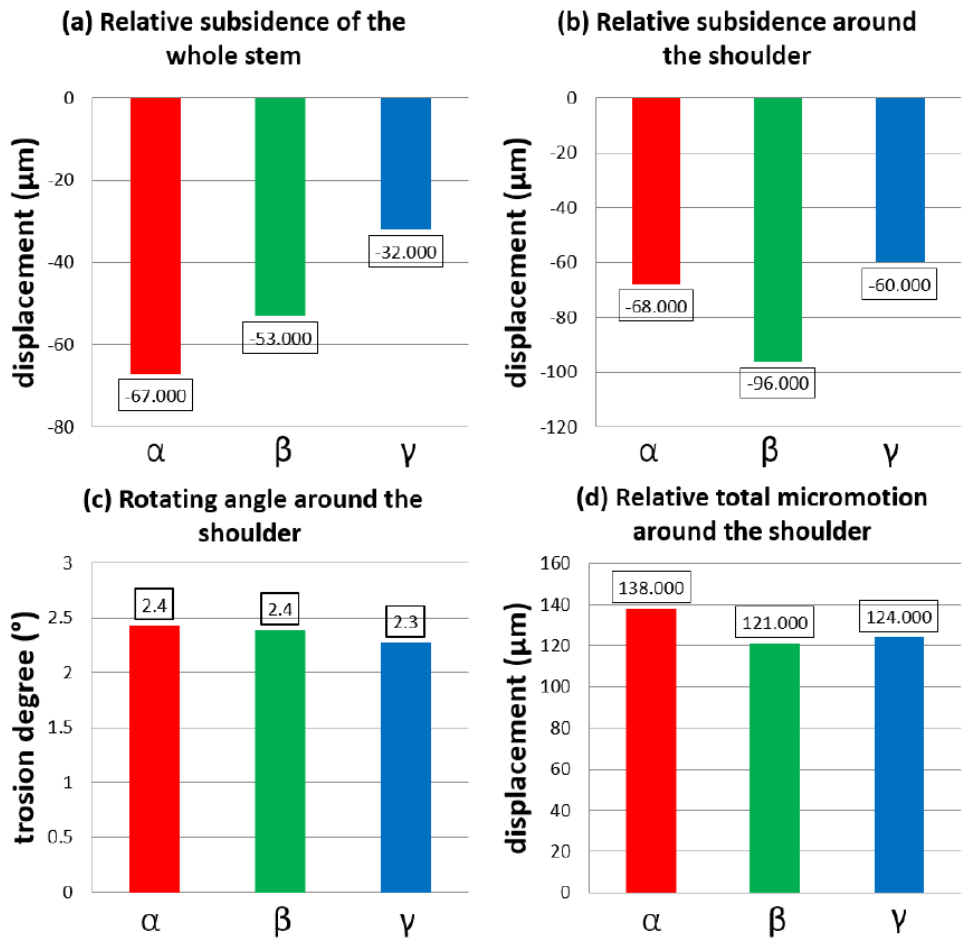


Figure 5: Parameters related to primary stability.

the bone. In this simulation, rotating angle is almost same observed in three stems, suggesting very similar torque loading probably, thus similar torsional stability.

Effenberger assumed that cementless stem is fixed at metaphyseal wall, moreover, proposed that proximal broad prosthesis with greater shoulder width introduced less surface load on prosthetic bearing to achieve a better primary stability [12]. According to this, one would consider that preserve α should subside more, due to less shoulder width. However, fixation at weak metaphyseal wall is not capable of affording enough resistance, especially for aged patients with osteoporosis. Matthias and Shigemura argued that a rectangular stem can achieve fixation at firm diaphysis by 4 corners locking into endosteal bone to provide a strong primary stability [7, 13]. In this case, since trochanteric shoulder is not a weight-bearing area, the effect of shoulder width is not important for the stability. This point matched the result of similar relative subsidence around the shoulder between three stems in this simulation.

Finally, the threshold of relative total micromotion for osseointegration is 100-200 μm . When it is more than this order, the bone on-growth will be inhibited. A layer of connective tissue is formed around the implant and results in a failure of aseptic loosening [6]. As a fundament to measure accurate micromotion, it is necessary for the method that accuracy should be at least less than 20 μm . In MF9.0, error of displacement value is 1 μm . It is precise enough to detect and compare the difference of relative micromotion by MF9.0 [14]. With regard to this simulation, Preserve α displayed maximum relative total micromotion of 138 μm , while preserve γ also gave rise to micromotion of 124 μm . The difference was slight. All stems subside within the upper threshold for adequate bone on-growth on stem surface. It suggested the new design, preserve α possesses a very similar primary stability which supports the bone on-growth process for long-term stability with conventional design of Zweymüller cementless stems.

5. CONCLUSIONS

This computational simulation study suggested that the trochanteric shoulder of Zweymüller stem is not mainly responsible for primary stability, due to the fixation mainly achieved at the diaphysis and metaphyseal-diaphyseal junction by the rectangular cross-section and the tapered stem. Bone on-growth during torsion and compression also would not be inhibited on the shoulderless stem. Hence, the

shoulderless design, Preserve α , would be acceptable in total hip arthroplasty. This could be an instruction to develop new design of cementless design to achieve less invasive surgery and also obtain excellent duration.

REFERENCES

- [1] Lafforgue P. Pathophysiology and natural history of avascular necrosis of bone, *Joint Bone Spine* 2006; 73: 500-507.
<https://doi.org/10.1016/j.jbspin.2006.01.025>
- [2] Guerado E, Caso E. The physiopathology of avascular necrosis of the femoral head: an update, *Injury-International Journal of the Care of the Injured* 476 (2016) S16-S26.
[https://doi.org/10.1016/S0020-1383\(16\)30835-X](https://doi.org/10.1016/S0020-1383(16)30835-X)
- [3] Khanuja HS, Vakili JJ, Goddard MS, Mont MA. Cementless femoral fixation in total hip arthroplasty, *JBJS* 2011; 93: 500-509.
<https://doi.org/10.2106/JBJS.J.00774>
- [4] Zweymüller K, Semlitsch M. Concept and material properties of a cementless hip prosthesis system with Al₂O₃ ceramic ball heads and wrought Ti-6Al-4V stems // Concept and material properties of a cementless hip prosthesis system with Al₂O₃ ceramic ball heads and wrought Ti-6Al-4V stems, *Archives of orthopaedic and traumatic surgery* 1982; 100: 229-236.
<https://doi.org/10.1007/BF00381662>
- [5] Sugiyama H, Whiteside LA, Engh CA, Sugiyama H, Whiteside LA, Engh CA. Torsional fixation of the femoral component in total hip arthroplasty. The effect of surgical press-fit technique, *Clinical orthopaedics and related research* 1992; 187-193.
<https://doi.org/10.1097/00003086-199202000-00027>
- [6] Sugiyama H, Whiteside LA, Kaiser AD, Sugiyama H, Whiteside LA, Kaiser AD. Examination of rotational fixation of the femoral component in total hip arthroplasty. A mechanical study of micromovement and acoustic emission, *Clinical orthopaedics and related research* 1989; 122-128.
<https://doi.org/10.1097/00003086-198912000-00014>
- [7] Shigemura T. The Trochanteric Wing of the Zweymüller Femoral Stem does Not Affect Rotational Stability: An Experimental Study Using a Resin Bone Model, *IJCEMS* 2017; 3: 66.
<https://doi.org/10.11648/j.ijcems.20170305.13>
- [8] Kolb A, Gröbl A, Schneckener CD, Chiari C, Kaider A, Lass R, Windhager R. Cementless total hip arthroplasty with the rectangular titanium Zweymüller stem: a concise follow-up, at a minimum of twenty years, of previous reports, *JBJS* 2012; 94: 1681-1684.
<https://doi.org/10.2106/JBJS.K.01574>
- [9] Keyak JH, Rossi SA, Jones KA, Skinner HB, Keyak JH, Rossi SA, Jones KA, Skinner HB. Prediction of femoral fracture load using automated finite element modeling, *J Biomech* (1998 // 1997); 31: 125-133.
[https://doi.org/10.1016/S0021-9290\(97\)00123-1](https://doi.org/10.1016/S0021-9290(97)00123-1)
- [10] Bessho M, Ohnishi I, Matsuyama J, Matsumoto T, Imai K, Nakamura K. Prediction of strength and strain of the proximal femur by a CT-based finite element method, *Journal of biomechanics* 2007; 40: 1745-1753.
<https://doi.org/10.1016/j.jbiomech.2006.08.003>
- [11] Bergmann G, Bender A, Dymke J, Duda G, Damm P. Standardized Loads Acting in Hip Implants, *PLOS ONE* 2016; 11: e0155612.
<https://doi.org/10.1371/journal.pone.0155612>
- [12] Effenberger H, Heiland A, Ramsauer T, Plitz W, Dorn U. A model for assessing the rotational stability of uncemented femoral implants, *Archives of Orthopaedic and Trauma*

- Surgery 2001; 121: 60-64.
<https://doi.org/10.1007/s004020000215>
- [13] Flury MP, Schmoelz W, Schreiber U, Goldhahn J. Biomechanical testing of rectangular humeral shaft prosthesis: higher torsional stability without increased fracture risk, Archives of Orthopaedic and Trauma Surgery 2011; 131: 267-273.
<https://doi.org/10.1007/s00402-010-1170-8>
- [14] Viceconti M, Muccini R, Bernakiewicz M, Baleani M, Cristofolini L, Viceconti M, Muccini R, Bernakiewicz M, Baleani M, Cristofolini L. Large-sliding contact elements accurately predict levels of bone-implant micromotion relevant to osseointegration // Large-sliding contact elements accurately predict levels of bone-implant micromotion relevant to osseointegration, Journal of biomechanics 2000; 33: 1611-1618.
[https://doi.org/10.1016/S0021-9290\(00\)00140-8](https://doi.org/10.1016/S0021-9290(00)00140-8)

Received on 11-04-2021

Accepted on 27-05-2021

Published on 05-06-2021

DOI: <http://dx.doi.org/10.12974/2313-0954.2021.08.1>

© 2021 Wu and Todo; Licensee Savvy Science Publisher.

This is an open access article licensed under the terms of the Creative Commons Attribution Non-Commercial License (<http://creativecommons.org/licenses/by-nc/3.0/>) which permits unrestricted, non-commercial use, distribution and reproduction in any medium, provided the work is properly cited.